Jonge, C. de, Stadnitskaia, A., Fedotov, A., & Sinninghe Damsté, J.S. (2015). Impact of riverine suspended particulate matter on the branched glycerol dialkyl glycerol tetraether composition of lakes: The outflow of the Selenga River in Lake Baikal (Russia). *Organic Geochemistry*, 83-84, 241-252

Published version: dx.doi.org/10.1016/j.orggeochem.2015.04.004

Impact of riverine suspended particulate matter on the branched glycerol dialkyl glycerol tetraether composition of lakes: The outflow of the Selenga River in Lake Baikal (Russia)

Cindy De Jonge[a*], Alina Stadnitskaia[a], Andrey Fedotov[b], Jaap S. Sinninghe Damsté[a,c]

[a]*Department of Marine Organic Biogeochemistry, NIOZ Royal Netherlands Institute for Sea Research, PO Box 59, 1790 AB Den Burg (Texel), The Netherlands*

[b]*Limnological Institute, Siberian Branch of the Russian Academy of Sciences, Irkutsk, Russian Federation*

[c]*Department of Earth Sciences, Faculty of Geosciences, Utrecht University. Budapestlaan 4, 3584 CD Utrecht, The Netherlands*

* Corresponding author; *E-mail address*: dejonge.cindy@gmail.com (C. De Jonge).

ABSTRACT

Branched glycerol dialkyl glycerol tetraethers (brGDGTs) are bacterial membrane lipids occurring in several environments, including soils, rivers and lakes, whose distribution varies with temperature and pH, although this dependence is apparently not the same for the different producing environments. Mixing of brGDGT sources may thus complicate palaeoenvironmental reconstruction. The extent to which brGDGTs in a lake outflow reflect the brGDGT distribution delivered by upstream rivers was studied for Lake Baikal (Russia), one of the largest freshwater lakes worldwide. Fifteen brGDGTs were quantified in suspended particulate matter (SPM) of the Selenga River and its outflow in the lake. The river and lake SPM had rather different brGDGT distributions. The riverine brGDGT distribution was still apparent in the SPM of the lake surface water 5 km from the river mouth, but shifts in the brGDGT distribution were already apparent in the SPM of the surface water after 1 km. Based on the brGDGT distributions of the SPM of the Selenga outflow and that of the lake, conservative mixing between the river and the lake brGDGT distributions could not fully explain the observed shifts in brGDGT distributions. Both preferential degradation and in-situ production of brGDGTs in the surface and, especially, bottom water of the river outflow were potentially responsible. This implies that a riverine lipid distribution delivered to a lake can be modified prior to being transported downstream. The lacustrine brGDGT distribution, that possibly reflected a mixture of mountainous and Selenga River SPM, was not recognized in downstream Yenisei River SPM. The watershed of Lake Baikal thus does not seem to contribute to the brGDGTs transported to the marine system. As many large rivers have major lakes in their watershed, this has implications for palaeoclimate reconstruction from river fan sediments globally.

KEYWORDS

brGDGTs, 6-methyl, in-situ production, degradation, Selenga River, Lake Baikal

1. Introduction

Branched glycerol dialkyl glycerol tetraethers (brGDGTs) are bacterial membrane lipids found in a variety of settings: soils, lacustrine and marine suspended particulate matter (SPM) and sediments and hotsprings. Their source organisms probably fall within the Acidobacteria, based on environmental (Weijers et al., 2009; Peterse et al., 2010) and culture studies (Sinninghe Damsté et al., 2011; 2014). Their main application is as palaeoclimate proxies. In a dataset of global soils, the structural diversity of the brGDGT components was shown to correlate with the prevailing soil pH and mean annual air temperature (MAAT; Weijers et al., 2007a). Nine brGDGT components were described that possess 4 to 6 methyl substituents (branches) on the linear C_{28} alkyl chains (Sinninghe Damsté et al., 2000) and contain up to two cyclopentyl moieties formed by internal cyclization (Fig. 1; Schouten et al., 2000; Weijers et al., 2006). The cyclization of branched tetraethers (CBT) and methylation of branched tetraethers (MBT) are two brGDGT indices (Weijers et al., 2007a) that have been successfully applied to reconstruct the palaeoclimatic changes in palaeosoils (e.g. Peterse et al., 2011), speleothems (Blyth and Schouten, 2013), lake sediments (e.g. Niemann et al., 2012), but initially in marine sediments (e.g. Weijers et al., 2007b; Bendle et al., 2010). Prior to their incorporation into marine and lacustrine sediments, they were understood to be eroded from soils and transported by rivers through upstream lakes. The brGDGT distribution was thus assumed to reflect the distribution present in watershed soils and to remain unaltered during this process.

Contrasting brGDGT distributions between rivers, lakes and their surrounding soils provided the first indications for in-situ production of brGDGTs in freshwater aquatic systems (e.g. Tierney and Russell, 2009). Although the temperature dependence is different from that in soils, the distribution of aquatic brGDGTs in lakes also varies with prevailing MAAT, and to some extent with depth and pH (e.g. Tierney et al., 2010; Pearson et al., 2011; Sun et al., 2011; Loomis et al., 2012, 2014a). There is thus a growing body of evidence supporting in-situ production of brGDGTs in lakes, but the niche of the source organism has not been constrained. The concentration of lacustrine brGDGTs was shown to increase below the lake thermocline, pointing towards a preference for environments with low O_2 concentration (e.g. Sinninghe Damsté et al., 2009; Buckles et al., 2014a). However, a recent study of brGDGTs in a temperate lake (Loomis et al., 2014b) found that brGDGTs were produced throughout the water column. Further possible mechanisms influencing the brGDGT distributions are shifts in bacterial community, possibly prompted by a large shift in nutrients or by the transition between river and lake biomes (Loomis et al., 2014b and references therein). Although in-situ production of brGDGTs has been described to occur in rivers (e.g. Kim et al., 2012; Zell et al., 2013, 2014; De Jonge et al., 2014a), a lacustrine in-situ produced distribution may be significantly different from that of its inflowing river (Tierney and Russell, 2009; Buckles et al., 2014b). As large lakes are often present in large river drainage basins, lacustrine in-situ production may result in the introduction of lacustrine brGDGTs in downstream rivers and ultimately in marine sediments. Large lakes in the drainage basin of river systems may thus have an effect on palaeoclimate brGDGT reconstruction for river fan marine sediments.

The aim of this study was to investigate the extent to which the brGDGT distribution delivered by a river can propagate in a large lake and to compare this effect with the brGDGT distribution exported from the lake by river outflow. Furthermore, we tried to constrain the environmental parameters that influence lacustrine in-situ production of brGDGTs. Although in-situ production of brGDGTs in lakes has been extensively documented (e.g. Tierney and Russell, 2009; Loomis et al., 2011, 2014b; Buckles et al., 2014a), this is the first study to evaluate the delivery and export of riverine brGDGTs toand from a lake system. Furthermore, the above previous studies are all based on a dataset of nine brGDGTs, as the analytical procedure used did not allow separating the recently described 6-Me brGDGTs (De Jonge et al., 2013). The abundance of these novel brGDGTs wasrecently shown to be high in a Siberian River system (De Jonge et al., 2014a) and to be highly variable in a set of globally distributed soils (De Jonge et al., 2014b).

This study describes the full suite of fifteen brGDGTs in a major river (Selenga River) that drains northern Mongolia and southern Siberia before and after its inflow to the world’s largest freshwater lake (Lake Baikal). We evaluate the brGDGT concentration and distribution in the Selenga River outflow, where in-situ production and preferential degradation could possibly affect the lacustrine brGDGT distributions. Furthermore, the distribution exported from the lake was compared with the brGDGT distribution in both Selenga River and the mountainous Irkut River, to evaluate whether or not riverine brGDGTs alone could explain the lacustrine brGDGT signature exported.

2. Geographical setting

The Selenga River originates in the mountainous parts of Mongolia, draining large parts of Mongolia and southern Siberia (442 000 km^2; Fig. 2b). It is the main tributary of Lake Baikal, with a drainage area 82% of the total drainage area of the lake. It transports 57.8 km^3/yr, which accounts for ca. 50% (Votintsev et al., 1985) of the total water input to the lake. Furthermore, it contributes ca. 80% of the total suspended solids delivered by the tributaries to the lake (Votintsev et al., 1985). The other tributaries (Fig. 2b) drain the steep, mountainous watershed that borders the lake on the North and the East. The lake is one of the largest in the world, containing ca. 20% of the Earth's fresh liquid surface water (23,000 km^3). The lake water is well mixed and aerated. The chemical and biological parameters of the Selenga River outflow have been studied by Maksimenko et al. (2008) and Sorokovikova et al. (2012). The mixing zone was described to be biologically very active, fueled by the riverine NO_3^- and PO_4^{3-}. Based on changes in water chemistry and the phyto- and bacterioplankton, the latter authors concluded that, during the summer months, the mixing zone extends from 1–3 km downstream off the Selenga River mouth, after which a lake signature dominates. Maksimenko et al. (2008) studied the microbial communities of the Selenga River outflow and concluded that a fully lacustrine composition occurs between 5 and 7 km downstream of the river mouth.

3. Material and methods

3.1. Collection of suspended particulate matter (SPM)

Table 1 lists the SPM samples investigated and the locations of the sampling stations are shown in Fig. 2. In July 2010, 100 l of Lake Baikal water was sampled from the shoreline at the point where it drains into the Angara River (Ba), further referred to as 'Lake Baikal outflow'). Between 10-20 L of the Selenga River outflow into Lake Baikal (SRM, S1, S3, S5, B1, B3, B5) were sampled later in July 2010 (Fig. 2a). It was sampled at the surface at the river mouth (Harauz tributary; SRM), and surface and bottom waters were sampled at 1 (S1 and B1), 3 (S3 and B3) and 5 km (S5 and B5) from the river mouth. The remaining samples were filtered using the same type of 0.7 μm GF/F glass fiber filters.

The bulk parameters of the riverine sites Y1, Y2, MIR and SR (Fig. 2) have been discussed by De Jonge et al., 2014a and the GDGT contents have been described by De Jonge et al. (submitted).

3.2. Lipid extraction and analysis

The freezedried filters were extracted using a modified Bligh and Dyer method as described by Pitcher et al. (2009). The samples were ultrasonically extracted 3x for 10 min using a MeOH/dichloromethane (DCM)/phosphate buffer 10:5:4 (v/v/v). The extract was separated into a core lipid (CL) fraction and intact polar lipid (IPL) fraction over a small silica column, using a procedure modified from Pitcher et al. (2009), using hexane/EtOAc (1:1, v/v) and MeOH as eluents. An aliquot of the IPL fraction was analyzed directly for CLs to check for potential carryover into the IPL fraction. In order to analyze IPLs as CLs, half of the extract was refluxed for a minimum of 2 h in 1.5 N HCl in MeOH. However, IPL-derived brGDGTs were often below the limit of detection, indicating that the amount of IPLs was insufficient for quantification, so we refrain from reporting the IPL brGDGTs composition of Selenga River and Lake Baikal. All brGDGTs were quantified against a known amount of C_{46} GDGT standard (Huguet et al., 2006) added to the CL fraction before filtration through a 0.45 µm PTFE filter and to the IPL fraction before the separation preceding the acid hydrolysis.

Fractions were analyzed using high performance liquid chromatography-atmospheric pressure chemical ionization-mass spectrometry (HPLC-APCI-MS), as described by De Jonge et al. (2014a). Detection was achieved in selected ion monitoring mode (SIM; Schouten et al., 2007) using *m/z* 744 for the internal standard, m/z 1292 for crenarchaeol and m/z 1050, 1048, 1046, 1036, 1034, 1032, 1022, 1020 and 1018 for brGDGTs. Agilent Chemstation software was used to integrate peak areas in the mass chromatograms of the $[M+H]^+$ions.

3.3. Calculation of GDGT-based ratios and proxies

The isomer ratio (IR) represents the fractional abundance of the penta- and hexamethylated 6-methyl (6-Me) brGDGTs vs. the total penta- and hexamethylated brGDGTs (modified after De Jonge et al., 2014a):

IR = (IIa’,b’,c’+IIIa’,b’,c’)/(IIa,b,c+IIIa,b,c+IIa’,b’,c’+IIIa’,b’,c’) 1

The roman numerals refer to the GDGTs indicated in Fig. 1. The index includes the non-cyclopentane containing and the cyclopentane containing components of brGDGTs II, III, II' and III'.

The branched and isoprenoid tetraether (BIT) index was calculated according to Hopmans et al. (2004):

$$\text{BIT index} = (Ia+IIa+IIIa+IIa'+IIIa')/(Ia+IIa+IIIa+IIa'+IIIa'+IV) \tag{2}$$

Ia, IIa, IIIa, IIa' and IIIa' are brGDGTs and IV is the isoprenoid GDGT (iGDGT) crenarchaeol, a source-specific GDGT for mesophilic Thaumarchaeota (Sinninghe Damsté et al., 2002; Pearson et al., 2004).

We calculated a reconstructed pH using the modified cyclization of branched tetraether CBT' index (De Jonge et al., 2014b):

$$CBT' = {}^{10}\log[(Ic+IIa'+IIb'+IIc'+IIIa'+IIIb'+IIIc')/(Ia+IIa+IIIa)]. \tag{3}$$

$$pH = 7.15 + 1.59 \times CBT' \tag{4}$$

Mean summer temperature (MST) is calculated as an approximation for the summer lake water temperature recorded by aquatic brGDGT distributions. To this end, we applied the calibration developed by Pearson et al. (2011):

$$MST\ (°C) = 20.9 + 89.1 \times [Ib] - 12 \times ([IIa] + [IIa']) - 20.5 \times [IIIa] \tag{5}$$

Here, we explicitly state that the fractional abundances of IIa and IIa' have to be summed, as these brGDGTs co-eluted under the chromatographic conditions used by Pearson et al. (2011). However, conditions did allow separation of brGDGTs IIIa and IIIa', and only the first eluting one (IIIa) was used in the calibration dataset (E. Pearson, personal communication). The square brackets in Eq. 5 indicate that we used the fractional abundance, i.e. the value relative to the sum of all the brGDGTs (Ia+Ib+Ic+IIa+IIa'+IIb+IIb'+IIc+IIc'+IIIa+IIIa'+IIIb+IIIb'+IIIc+IIIc').

3.4. Environmental parameters and bulk geochemical analysis

The pH and temperature of the river and lake water were measured immediately after sampling, except for the sample SR, whose parameters were measured after transport. The particulate organic carbon (POC) and $\delta^{13}C_{POC}$ content of the river and lacustrine SPM samples were measured on the filter using a Flash 2000 Organic Elemental Analyzer.

3.5. Numerical analysis

Principal component analysis (PCA) based on the correlation matrix was performed using the R software package for statistical computing. We performed an unconstrained Q-mode PCA on the standardized relative brGDGT values in SPM from the Selenga River, Lake Baikal and mountainous Irkut River, using 11 brGDGTs. The brGDGTs IIc, IIIc, IIc' and IIIc' were excluded from this analysis, as they were absent from 4 to 7 sample sites. The brGDGT scores were calculated proportional to the eigenvalues, and the site scores were calculated as the weighted sum of the species scores. The environmental parameters (point measurement of water pH and temperature) were plotted a posteriori in the resulting ordination space, in case a significant correlation ($p>0.05$) with the principal components (PCs) was present.

4. Results

The brGDGT distribution of the SPM in the Selenga River was determined, before and after its outflow into Lake Baikal. The river SPM was collected ca. 150 km before its inflow into the lake (SR). The transect in the outflow comprised 7 sites, the Selenga River Mouth (SRM), the surface water at 1, 3 and 5 km from the outflow (S1, S3, S5) and the bottom water at 1, 3 and 5 km from the outflow (B1, B3, B5). A shoreline SPM sample from a site in Lake Baikal (Ba) not directly influenced by the river, close to the point where the lake water flows into the Angara River, allowed contrasting the Lake Baikal distribution exported with the Yenisei river system further downstream, before (Y1) and after (Y2) the contribution of the Angara River. Furthermore, the brGDGT distribution of the SPM of a mountainous river (i.e. the Irkut River; MIR) was evaluated to constrain the influence that similar mountainous rivers that drain into the lake may have on the lacustrine brGDGT distribution. The sites and bulk parameters for the organic matter (OM) in SR, MIR, Y1 and Y2 have been reported by De Jonge et al. (2014a), while the GDGT concentrations and distributions have been reported previously by De Jonge et al. (submitted).

4.1. Environmental and bulk OM parameters

The Selenga River, Lake Baikal and the Mountain River are contrasting waterbodies, as reflected in both the temperature and bulk POC content, and to a lesser extent in the pH and bulk $\delta^{13}C_{POC}$ values (Table 1). The inflow of Selenga River into the lake is characterized by a strong gradient in water temperature (Fig. 3A), decreasing from 25 °C in the river and 22.5 °C at the river mouth to 11.3 °C at S5. The bottom water is on average 6°C colder than the surface water. The coldest water in the Selenga outflow system (5.2 °C) was the bottom water at 5 km distance. The Lake Baikal outflow sample (Ba) had a temperature of 6.7 °C. The pH remained more constant in the outflow system (Fig. 3B), with a river water pH of 8.4, while the outflow system had a pH that varied around 8.0 pH units. The POC varied between 6.4 and 1.1 mg/l, with the highest values in the river. A clear downstream trend was observed (Fig. 3C), POC decreasing as the river flows further in Lake Baikal. The POC content of the bottom water (2.5-1.1 mg/l) was always lower than for the corresponding surface water, although the difference was most pronounced near the shore. The $\delta^{13}C_{POC}$ values (Fig. 3D) showed that the lake bottom water to have an increasingly negative value downstream (down to -29.7 ‰) compared with the river SPM (-27.6 ‰). Surface water in the outflow system also had more negative value of $\delta^{13}C_{POC}$ than the river, except for the sites 3 and 5km from the river mouth, that had a comparable value as the river mouth (-28.6 to -28.4 ‰). The shoreline lake site had an offset, much less negative $\delta^{13}C_{POC}$ value (-24.0 ‰). The mountainous Irkut River differed from the lowland Selenga River, as it has the lowest POC content in the (0.1 mg/l), a much lower pH (5.6) and a lower water temperature (10.8°C). On the other hand, the $\delta^{13}C_{POC}$value of -27.8 ‰ was comparable to that in the Selenga River. The Yenisei River before and after the inflow of the Angara River had a neutral pH (7.5-7.9), a temperature between 11 and 12 °C, and the one measured $\delta^{13}C_{POC}$ value (-30.5 ‰) was slightly more negative than for both the Selenga River and Lake Baikal systems.

4.2. GDGT amounts and distribution

The amounts and distribution of crenarchaeol and the brGDGTs are listed in Table 2. SPM of the Selenga River and the river mouth had a low amount of crenarchaeol (0.3-0.5 μg/g POC; Fig. 4B), which increased slightly in the outflow surface water (up to 0.5 μg/g POC). SPM of the bottom waters contained a higher amount of crenarchaeol (0.9-3 μg/g POC), with the highest amount 3 km from the delta. The lake outflow and the Yenisei River SPM had a low crenarchaeol concentration, between 0.2 and 0.3 μg/g POC. The amount of brGDGTs was highest at the Selenga River Mouth (10-12 μg/g POC; Fig. 4A), substantially higher than in the river itself (4 μg/g POC), although this was measured in a different month and can thus not be directly compared. The brGDGT concentration decreased in the surface water of the outflow system to 0.6 μg/g POC. The mountainous Irkut River had the highest POC-normalized brGDGT concentration at 15 μg/g POC. The brGDGTs in the bottom water varied between 2 and 10 μg/g POC, with the highest values 3 km from the Selenga River Mouth. The lake outflow had the lowest amount of brGDGTs, with 0.1 μg/g POC. The abundance in the Yenisei River SPM varies between 10 and 21 μg/g POC (De Jonge et al., 2014b).

Typical examples of brGDGT distributions in the SPM are shown in Fig. 5. The distribution in the Selenga River Mouth (Fig. 5A) was dominated by 6-Me pentamethylated brGDGTs, and relatively abundant cyclopentane-containing brGDGTs (17%). It was markedly different from that in the lake outflow (Fig. 5E), which was dominated by 5-Me and 6-Me hexamethylated brGDGTs, and a lower contribution of cyclopentane-containing brGDGTs (5%). The brGDGTs in the Selenga outflow seemed to have intermediate distributions (Fig. 5B-D), while the mountain river had a distribution comparable with that of the lake outflow (Fig. 5E-F). The distribution in the Yenisei River samples (Fig. 5G-H) was dominated by 6-Me brGDGTs, the hexamethylated compounds in particular dominated.

To study the variance in the brGDGT distribution of the lake and the rivers in its watershed (Selenga and Irkut), a PCA was performed, based on the fractional abundances of brGDGTs in the Selenga River, Lake Baikal and the mountainous Irkut River (n = 10). Most brGDGTs containing two cyclopentanes, i.e. IIc, IIc', IIIc and IIIc' were excluded, as they were absent from 4 to7 samples. The first three PCs accounted for a large part of the variance (almost 90%), being 41%, 25% and 21%, respectively. The first PC highlighted the correlation of a group of minor brGDGTs with positive values on PC1 (Ib, Ic, IIb, IIIb, IIa', IIb', IIIb') and, to a lesser extent, brGDGT Ia (Fig. 6A). The brGDGTs IIa and IIIa had negative values on PC1. PC2 revealed that brGDGT IIIa', and to a lesser extent IIa' and IIb', showed a negative correlation with Ic, IIb and IIIb (Fig. 6A). BrGDGT Ia had a positive score on PC3, while IIIb and IIIb' had a negative score (Fig. 6C). The similarity in the brGDGT distributions at each site could be evaluated comparing their scores on the first three PCs. The similar scores for the Selenga River, Selenga River Mouth and the surface water 1 km from the river mouth, indicated that the brGDGT distributions were similar (Fig. 6B, D). Moving downstream (S3, S5) the scores on PC1 decreased, and the scores on PC2 and, especially, PC3 increased. The distribution for S3 (Fig. 5B) indeed showed increased fractional abundances of the 5-Me brGDGTs Ia, IIa and IIIa, at the expense of decreased fractional abundances of 6-Me brGDGTs. This was also apparent from the IR ratio (Table 2; Fig. 8A) that decreased downstream in the Selenga outflow surface water. Compared with the overlying surface water, SPM of the bottom water had an increased score on PC2, reflecting a decrease in brGDGT IIIa', coupled with an increase in brGDGTs IIa and IIIa, that dominated the distributions of B3 and B5, respectively (Fig. 5C, 5D). This resulted in lower IR values (Table 2; Fig. 8A) of the bottom water vs. the overlying surface water. The brGDGT distribution in the lake outflow, was most similar to that in the mountainous Irkut River, as reflected in the similar scores on PC1 and PC3. However, on PC2, the lake outflow sample had more negative values, caused by a larger fractional abundance of IIIa and IIIa' (Fig. 5E).

The point measurement of water temperature had a significant correlation with the PCs ($p<0.05$) and were plotted a posteriori in the PCA. The water temperature values had a positive score on PC1, and a negative one on PC2. The point measurements of water pH showed no significant correlation with the PCs ($p < 0.05$).

5. Discussion

5.1. Characteristics of Selenga River outflow

During the sampling period (September 2011), the Selenga outflow system was characterized by a warmer surface layer that extended to at least 5 km in Lake Baikal. Although a strong thermal bar is usually present during the start of the summer (Sorokovikova et al., 2012), its stability generally breaks down later in summer. The temperature profile shows that there was no complete stratification of the Selenga River outflow water during the sampling, and partial mixing caused the bottom water temperature to warm, especially near the shoreline (Fig. 3A). The $\delta^{13}C_{POC}$ values of the Selenga River and River Mouth SPM (-27.5 to -28.5‰) are indicative of a dominant terrigenous signature, probably derived from soil or terrigenous vegetation (typically -27‰; Michener and Lajtha, 2007). Although large blooms of phytoplankton were described to be present in the mixing zone of the river inflow (Sorokovikova et al.; 2012), this apparently has little impact on the $\delta^{13}C_{POC}$ values in the Selenga outflow surface SPM (Fig. 3D). This may be due to the similar $\delta^{13}C$ signature of the lake phytoplankton and the terrigenous organic matter (OM), as the former varies between -27 and -29.5‰ (Yoshii et al., 1999). Bottom water SPM, however, shows increasingly negative $\delta^{13}C_{POC}$ values, possibly reflecting the slightly more negative $\delta^{13}C_{POC}$ values of lacustrine phytoplankton, compared to the Selenga River, as the highest abundance of lake phytoplankton was in the bottom waters at 5 km distance (Sorokovikova et al., 2012). Alternatively, this may be caused by a shift in the microbial community (Maksimenko et al., 2008; Sorokovikova et al., 2012), possibly with an increased contribution of organotrophic bacteria. Increased amounts of such bacteria in the bottom water have been described, with maximum abundance in the bottom water at 5-10 (Maksimenko et al., 2008) or 14 km from the Selenga River mouth (Sorokovikova et al., 2012). They may thrive on the easily hydrolysable OM entering the near-bottom layers from decomposition of the spring algae (Votintsev et al., 1975). The shoreline lake SPM probably does not reflect an open water lacustrine end member. Here, the POC is substantially more enriched in ^{13}C, but this probably reflects the contribution of a isotopically enriched OM derived from macrophytes ($\delta^{13}C$ between -19 and -5‰; Yoshii, 1999) and benthic algae ($\delta^{13}C$ between -12 and -5‰; Yoshii, 1999), as the SPM was sampled in a shallow setting.

5.2. Changing GDGT abundance in the Selenga River outflow

As the Selenga River is the main source for SPM in Lake Baikal, its iGDGT and brGDGT distribution is expected to contribute to the lacustrine GDGT signature. The iGDGT crenarchaeol is present only in a low abundance in the river water. As it is a tracer for mesophilic Thaumarchaeota (Sinninghe Damsté et al., 2002), this fits with a reported absence of archaea from the river water (Maksimenko et al., 2008). The amount of archaea increases in the lake (Maksimenko et al., 2008) and the increase is mimicked by a slight increase in the amount of crenarchaeol in the outflow surface water (Fig. 4B). The downstream trend in the brGDGT concentration in the outflow is different, being highest in the river mouth, and decreasing in the surface water of the river outflow system (Fig. 4A). The decrease in brGDGT concentration in an outflow system is similar to studies where brGDGTs are traced in river outflows in marine environments (e.g. Hopmans et al., 2004; Zell et al., 2014; De Jonge et al., submitted). The decrease in POC-normalized concentration of riverine brGDGTs after their inflow into Lake Baikal can be a result of dilution in the lacustrine environment due to in-situ produced OM, or to degradation in the active biological system of the river outflow (Maksimenko et al., 2008; Sorokovikova et al., 2012). However, the brGDGT concentration in the bottom water 3 and 5 km from the river mouth, exceeds the surface water concentration. At 3 km from the outflow, the crenarchaeol concentration in the bottom water also exceeds the concentration in the surface water, (i.e. a fivefold increase).

As no significant decrease in POC concentration was observed at B3 and B5 (Fig. 3C), we infer that the increase in GDGTs at these sites is not an artifact of the normalization to POC. Although they are produced by different source organisms, both crenarchaeol and brGDGTs have been described to be produced in-situ in the lacustrine environment. Crenarchaeol was shown to be an abundant compound in the marine environment (Sinninghe Damsté et al., 2002), but also in most medium-sized and large lakes studied (Blaga et al., 2009), as it is produced by marine and freshwater Thaumarchaeota (e.g. Sinninghe Damsté et al., 2002, Pearson et al., 2004). These NH_3 oxidizing Archaea have a preferred niche in the oxycline/thermocline and nitrocline of the water column of lakes (e.g. Pouliot et al., 2009; Llirós et al., 2010; Auguet et al., 2011; Blaga et al., 2011; Schouten et al., 2012; Woltering et al., 2012; Buckles et al., 2013), where they can outcompete NH_3-oxidizing bacteria. The presence of an increased supply of decomposed algal matter in near-bottom water layers, resulting in increased NH_3 concentration (e.g. Jewell and McCarty, 1971), can possibly fuel the crenarchaeol production in these deeper layers. Also in-situ production of brGDGTs has been observed in lacustrine environments, based on shifts in the distribution and increased abundance (e.g. Tierney and Russell, 2009). BrGDGT producers in soils are believed to be heterotrophic bacteria (e.g. Pancost and Sinninghe Damsté, 2003; Weijers et al., 2010). Thus, the in-situ production at these sites can possibly be linked to enhanced heterotrophic activity in the bottom water. Indeed, the amount of organotrophic bacteria was shown to be slightly increased in the bottom water at 5-10 km from the Selenga River Mouth (Maksimenko et al., 2008).

To trace the transport of bacterial OM (soil-derived and/or river-derived) in the marine system, the BIT index was developed (Hopmans et al., 2004), expressed as the abundance of the non-cyclopentane containing brGDGTs, relative to the abundance of crenarchaeol. In the Selenga outflow, the concentration of brGDGTs is the dominant driver for the changing BIT index (Fig. 4C), as it correlates with the amount of brGDGTs ($r^2 = 0.63$). The index decreases with increasing distance from the river mouth. The decrease is to be expected, and has been observed in front of several river outflows in the marine system (e.g. Hopmans et al., 2004; Zell et al., 2014; De Jonge et al., submitted). The slightly increased values in the bottom water reflect the increased amount of brGDGTs there compared with the surface outflow water. The value for the lake outflow (0.22), is lower than reported values for sediment cores from the lake, where Holocene values vary between 0.3 and 0.6 (Fietz et al., 2011), although the difference can still be related to interlaboratory differences that can influence the values obtained (Schouten et al., 2009, 2013). Overall, the brGDGT abundance decreases significantly in the river outflow, while the crenarchaeol abundance remains stable. However, in-situ production of both crenarchaeol and brGDGTs within the bottom water is likely. Based on the distance from the river mouth, the increase is possibly fueled by increased degradation of phytoplankton material in the bottom water (Maksimenko et al., 2008; Sorokovikova et al., 2012).

5.3. Changing brGDGT distributions in the outflow of Selenga River and Lake Baikal

The distribution in the Selenga River and the River Mouth is distinctly different from the shoreline lake SPM that is presumably transported further downstream to the Yenisei River (Fig. 5A, F). Downstream changes in the fractional abundance of all 15 brGDGTs can be seen in the distributions (e.g. Fig. 5A-E) and the PCA based on the fractional abundances (Fig. 6). To evaluate whether the downstream changes are due exclusively to linear mixing between a riverine (SRM) and lacustrine (Ba) endmember, we plotted the data in a triplot based on the fractional abundance of three major brGDGTs (Fig. 7). It captures the majority of the variance, as the three brGDGTs have high scores on the first three PCs (brGDGTs IIIa, IIIa' and Ia, respectively). In the case that linear mixing is the only mechanism causing the shift in brGDGT distribution in the Yenisei outflow, and if the two endmembers (lacustrine, riverine) are well represented by the Ba and SRM samples, distributions that result from conservative mixing of these endmembers alone should fall on the thick black line in Fig. 7. However, both surface and bottom water SPM along the Selenga outflow transect do not fall on this mixing line. Compared with the Selenga River Mouth, the surface outflow water shows a stepwise increase in the fractional abundance of IIIa, and a decrease for Ia and IIIa'. Bottom water SPM also shows an increase in IIIa (in B1, but especially B3 and B5) and a decrease in Ia and IIIa'. The increase in IIIa correlates well with a decrease in Ib, IIa' and IIb' (r^2 = 0.57, 0.90 and 0.96, respectively). Possible explanations for the offset from the linear mixing line are preferential degradation of a brGDGT pool that was enriched in the Ia, Ib, IIa', IIb' and IIIa', or the in-situ production of IIIa in the outflow. Although the brGDGT distribution in the river reflects a mixture dominated by in-situ produced brGDGTs, a small contribution from soil-derived brGDGTs could be present. As the riverine OM will be more easily degraded (e.g. Blair and Aller, 2012), a soil-derived brGDGT sub-pool could become more dominant during degradation of the OM delivered by the river. However, especially in the bottom water, in-situ production of brGDGTs is probable, based on the increased brGDGT concentration. In-situ production of brGDGTs in lacustrine systems has been described in several studies, both for the lake water column or sediments. Unfortunately, these studies do not allow discussing changes in the abundance of 5- and 6-Me brGDGTs separately, although the relative abundance of the 6-Me brGDGTs, expressed as the isomer ratio (IR, Eq. 1; Fig. 8A) shows strong changes downstream. The contrasting behavior of the 5- and 6-Me brGDGTs is also reflected in their dissimilar scores in the PCA (Fig. 6A, C) and ideally they should therefore be studied separately when discussing aquatic brGDGT distributions.

Loomis et al. (2014) have shown that cyclopentane-containing brGDGTs and penta- and hexamethylated brGDGTs can be produced in the water column of a temperate lake, both in the surface water and bottom water. A study (Buckles et al., 2014a) of the partially anoxic Lake Challa showed that penta- and hexamethylated brGDGTs were produced in the oxic part of the water column, but mainly in the suboxic part, and found some evidence suggesting their production in sediments.

Furthermore, the authors showed that in-situ production of IIIa (and/or IIIa') and IIb (and/or IIb') occurred in the Loch Lomond (Scotland), although they could not pinpoint whether the production was localized in the sediments or in the water column. Indications were also found for in-situ production of penta- and hexamethylated brGDGTs in the suboxic sediments of Sand Pond (USA; Tierney et al., 2012). Overall, previous studies agree on the production of highly methylated and cyclopentane-containing brGDGTs by brGDGT producing bacteria occupying a variety of niches within the lacustrine environment. This is in line with the postulated in-situ production of IIIa in the Selenga Outflow. As IIc, IIc', IIIc and IIIc' were below detection limit in 4-7 samples, an increase in their fractional abundance could not be established.

We have shown that the distribution in the Selenga River outflow cannot be explained solely by mixing of a riverine end member and a lacustrine endmember. However, the source of the brGDGT distribution in the lacustrine endmember (Ba) still remains to be constrained. Besides being in-situ produced, a second possible source for the brGDGT distribution in Lake Baikal is brGDGTs delivered by other rivers that account up to 50% of its water volume, and up to 20% of the total suspended solids (Votintsev et al., 1985). Although we did not sample the SPM from such rivers within the watershed, we sampled the brGDGTs in the headwater of Irkut River, a mountainous river in a nearby and similar location (Fig. 2), for which we postulate that it should approach the brGDGT distribution in the northern and eastern rivers of the watershed of the lake and in the headwaters of Selenga River. The distribution in the SPM of this mountainous river and that of the lacustrine endmember are rather similar (Fig. 5E, F), as confirmed by their similar scores on PC1 and PC3 (Fig. 6B, D). Although linear mixing (Fig. 7, dotted line) between the distributions in the mountain river and the Selenga River, approaches the lacustrine distribution, a small decrease in the fractional abundance of Ia and IIIa, or an increase in IIa', IIb' and IIIa' is needed to explain the distribution in the lake. Unfortunately, it is impossible to determine whether preferential degradation or in-situ production of brGDGTs is the more probable explanation.

Another issue is how the lake water affects the brGDGT composition of downstream Yenisei river water. The distribution in the latter (Figs. 5G-H; Fig. 7) is distinctly different from that of the lake outflow (Fig. 5E; Fig. 7) with a much larger fractional abundance of 6-Me brGDGTs. This dominance becomes even more evident after the inflow of the Angara River, that drains lake water into the Yenisei River. The signature of the latter (Figs. 5G-H; Fig. 7) is more similar to that of the Selenga River (Fig. 5A; Fig. 7). This indicates that riverine in-situ production of brGDGTs, a process reported to be dominant for brGDGT distribution in the whole Yenisei River (De Jonge et al., 2014b), already operates in the Angara River. This is confirmed by the two orders of magnitude higher concentration of brGDGTs in the Yenisei River SPM than in the lake. As the lacustrine brGDGT distribution is not present in downstream SPM, we postulate that brGDGTs sourced from the watershed of the lake, including the Selenga River watershed, should not contribute significantly to the brGDGT distribution transported by the Yenisei River and delivered to the marine system.

5.4. Environmental controls on brGDGT distributions in the Selenga River outflow

The lacustrine sedimentary brGDGT distribution of lakes covering a latitudinal or altitudinal range responds to overlying air temperature (e.g. Tierney et al., 2010; Sun et al., 2011; Pearson et al., 2011; Loomis et al., 2012) and to seasonal changes in water temperature (e.g. Loomis et al., 2014a). Similar to the soil calibrations, these authors found an increase in Ia in warmer lake settings, and a decrease of penta- and hexamethylated brGDGTs. Furthermore, some authors found evidence that pH has an influence on the brGDGT distributions (Tierney et al., 2010; Loomis et al., 2014a; Schoon et al., 2013), while others found no indication of this (Pearson et al., 2011; Loomis et al., 2014b).

The measured environmental parameters (point measurements of pH and water temperature) have been plotted a posteriori in the ordination space (Fig. 6A), in the case of significant correlation ($p < 0.05$) with the PC. The value of this vector in the ordination space is based on the correlations between the values of the environmental parameters at the sites, with the site scores on the PCs and thus revealing their relationship with individual brGDGTs. Their direction indicates for which samples their values are increased, and with which brGDGT correlations are present. The measured water temperature values correlated significantly with the site scores on the first two PCs ($p < 0.02$). The increase in fractional abundance of IIa and IIIa in the Selenga outflow results in a negative correlation with the measured water temperature as the temperature decreases strongly in the Selenga River outflow ($r^2 = 0.34$ and 0.64, respectively). The measured water temperature follows a positive correlation with the fractional abundance of IIa' and IIb' (r^2 = 0.75 and 0.59, respectively). The measured pH values do not correlate significantly with the main trends in the brGDGT distribution.

As the change in brGDGT distribution seems to be related to water temperature, we evaluate the performance of a MST calibration based on the fractional abundance of lacustrine brGDGTs (Pearson et al., 2011; Eq. 6). However, to date, no lake calibration has been based on the extended dataset of 15 brGDGTs. Although this calibration excluded IIIa' (E. Pearson, personal communication), it included the pentamethylated 6-Me brGDGTs, that vary strongly in the Selenga River outflow. The reconstructed MST for the outflow surface water varies between 18 and 20 °C (Fig. 8B). The bottom water values, except for sample B3 (17-19 °C; Fig. 8B), reflect the same temperature as the surface values, within the RSME of the calibration (2 °C; Pearson et al., 2011). As the absolute water temperature decreases from 25 to 12 °C (Fig. 3A), the reconstructed temperature values only give a muted response to this large decrease in temperature. The muted response to the temperature shift measured in-situ is a phenomenon also recognized by Loomis et al. (2014a). Although major shifts in the fractional abundance of the penta- and hexamethylated brGDGTs occur in the Selenga outflow, this is thus not reflected in the reconstructed temperature. This is caused by the combination of 5- and 6-Me pentamethylated brGDGTs. The Pearson et al. (2011) calibration is based on the air MST, that varies between 10.6 and 15.4 °C in the Lake Baikal watershed, based on 5 climate stations (De Jonge et al., 2014a). In this respect, the reconstructed MST overestimates the MST measured in the watershed.

Although the brGDGT distribution at B3 is generally comparable with that in the other river outflow samples, it results in a substantially lower reconstructed temperature (15 °C; decrease of 4 °C), because of the larger fractional abundance of IIa. This decrease in reconstructed temperature is not related to a decrease in water temperature (Fig. 3A). As strong shifts in the abundance of nutrients have shown to cause shifts in brGDGT distributions that are probably related to shifts in the microbial community (Loomis et al., 2014a), the low reconstructed temperature values can be due to the presence of a distinct brGDGT producing bacterial community associated with an increased amount of phytoplankton-derived detritus.

We also tested the performance of the most recent soil pH calibration (De Jonge et al., 2014b) in this aquatic setting. To this end, a pH reconstruction was performed using the CBT', a ratio based on a dataset where all 15 brGDGTs were quantified separately. The reconstructed pH (Eqs. 3 and 4) has absolute values (7-7.5) that only slightly underestimate the pH measured in the river and lake water (7.9-8.9), especially when taking the residual error of 0.5 pH units into account. The reconstructed pH shows a slight decrease in the Selenga outflow surface water, that is an intensified response compared with the measured values. In the outflow system, sample B3, with a reconstructed pH of 6.5 has the largest offset with the measured pH (7.9). The brGDGT signature at the site, which is most probably influenced by an in-situ produced brGDGTs, thus fails to reconstruct the in-situ measured pH. Furthermore, although the mountainous Irkut River has a lower pH than the lake, the brGDGT distributions are fairly similar. Overall, this environmental dataset indicates a limited influence of pH on the aquatic brGDGT distributions, as all reconstructed pH values vary around 7-7.5, and do not correlate with the measured values.

6. Conclusions

We have traced the Selenga River brGDGT signature during its outflow into Lake Baikal and compared the brGDGT signature with the outflow from Lake Baikal and the brGDGT distribution in the Yenisei River SPM. The signature for the Selenga River is characterized by a dominance of 6-Me brGDGTs IIa' and IIIa' (Selenga River endmember). Although the Selenga River delivers the largest part of the suspended matter to Lake Baikal, the brGDGT distribution delivered by it is drastically different from the lacustrine brGDGT distribution, that shows an increased amount of brGDGT IIa and IIIa (lacustrine endmember). As linear mixing of these two endmembers can not explain the shifts in the Selenga Outflow brGDGT distribution, we postulate that in-situ production of brGDGTs or preferential degradation takes place in the Selenga outflow. The presence of active archeael/bacterial communities in dynamic river outflow systems in lakes can thus possibly influence the brGDGT distribution encountered in lake sediments, especially as the extent of these outflow systems changes within and in between years. The brGDGT distribution of the lacustrine endmember can be produced in-situ in the lake, or can be caused by a contribution from brGDGTs derived from mountainous rivers in the Selenga watershed, that is dominated by non-cyclopentane containing penta- and hexamethylated brGDGTs (mountain river endmember).

Furthermore, the brGDGT distribution in the Yenisei River, both before and after the inflow of the Angara River that drains Lake Baikal, was studied. This distribution was found to be dissimilar to the lacustrine endmember, indicating only a limited contribution from the lacustrine brGDGTs to the Yenisei River distribution. The dominance of 6-Me brGDGTS, similar to the brGDGT distribution encountered in the Selenga River, indicated that the lacustrine brGDGT signature is overwritten by in-situ produced riverine brGDGTs (De Jonge et al., 2014a; submitted). The watershed of Lake Baikal thus does not contribute significantly to the brGDGT pool transported by the Yenisei River. Large lakes are a common feature in river watersheds globally and this study indicates that their presence can result in the absence of brGDGTs sourced in areas upstream of these lakes. This has to be taken into account when interpreting palaeoclimate reconstructions based on brGDGTs from river fan sediments. This study therefore has several implications for the use of lipid-based palaeoclimate proxies, both in lacustrine and marine sediments.

Acknowledgments

We acknowledge the helpful comments of two anonymous referees and the assistance of I. Tomberg (Limnological Institute, Irkutsk, Siberian Branch of Russian Academy of Science), who provided the filtered Selenga River transect SPM. The work was performed in the framework of the MOU between NIOZ and VNIIOkeangeologia (St. Petersburg, Russian Federation) for Arctic research. The study was funded by research project 819.01.013, financed by the Netherlands Organization for Scientific Research (NWO) and the European Research Council under the EU Seventh Framework Programme [FP7/2007-2013)/ERC grant agreement No. 226600].

References

Auguet, J.-C., Nomokonova, N., Camarero, L., Casamayor, E.O., 2011. Seasonal changes of freshwater ammonia-oxidizing Archaeal assemblages and nitrogen species in oligotrophic alpine lakes. Applied Environmental Microbiology 77, 1937–1945.

Bendle, J.A., Weijers, J.W.H., Maslin, M.A., Sinninghe Damsté, J.S., Schouten, S., Hopmans, E.C., Boot, C.S., Pancost, R.D., 2010. Major changes in glacial and Holocene terrestrial temperatures and sources of organic carbon recorded in the Amazon fan by tetraether lipids. Geochemistry Geophysics Geosystems 11, Q12007.

Blaga, C.I., Reichart, G.J., Heiri, O., Sinninghe Damsté, J.S., 2009. Tetraether membrane lipid distributions in water-column particulate matter and sediments: a study of 47 European lakes along a north–south transect. Journal of Paleolimnology 41, 523–540.

Blaga, C.I., Reichart, G.-J., Vissers, E.W., Lotter, A.F., Anselmetti, F.S., Sinninghe Damsté, J.S., 2011. Seasonal changes in glycerol dialkyl glycerol tetraether concentrations and fluxes in a perialpine lake: Implications for the use of the TEX_{86} and BIT proxies. Geochimica et Cosmochimica Acta 75, 6416–6428.

Blair, N.E., Aller, R.C., 2012. The fate of terrestrial organic carbon in the marine environment. Annual Review of Marine Science 4, 401–423.

Blyth, A.J., Schouten, S., 2013. Calibrating the glycerol dialkyl glycerol tetraether temperature signal in speleothems. Geochimica et Cosmochimica Acta 109, 312–328.

Buckles, L.K., Villanueva, L., Weijers, J.W.H., Verschuren, D., Sinninghe Damsté, J.S., 2013. Linking isoprenoidal GDGT membrane lipid distributions with gene abundances of ammonia-oxidizing Thaumarchaeota and uncultured crenarchaeotal groups in the water column of a tropical lake (Lake Challa, East Africa). Environmental Microbiology 15, 2445–2462.

Buckles, L.K., Weijers, J.W.H., Verschuren, D., Sinninghe Damsté, J.S., 2014a. Sources of core and intact branched tetraether membrane lipids in the lacustrine environment: Anatomy of Lake Challa and its catchment, equatorial East Africa. Geochimica et Cosmochimica Acta 140, 106–126.

Buckles, L.K., Weijers, J.W.H., Tran, X.-M., Waldron, S., Sinninghe Damsté, J.S., 2014. Provenance of tetraether membrane lipids in a large temperate lake (Loch Lomond, UK): implications for GDGT-based palaeothermometry. Biogeosciences 11, 5539-5563.

De Jonge, C., Hopmans, E.C., Stadnitskaia, A., Rijpstra, W.I.C., Hofland, R., Tegelaar, E., Sinninghe Damsté, J.S., 2013. Identification of novel penta- and hexamethylated branched glycerol dialkyl glycerol tetraethers in peat using HPLC–MS^2, GC–MS and GC–SMB-MS. Organic Geochemistry 54, 78–82.

De Jonge, C., Stadnitskaia, A., Hopmans, E.C., Cherkashov, G., Fedotov, A., Sinninghe Damsté, J.S., 2014a. In situ produced branched glycerol dialkyl glycerol tetraethers in suspended particulate matter from the Yenisei River, Eastern Siberia. Geochimica et Cosmochimica Acta 125, 476–491.

De Jonge, C., Hopmans, E.C., Zell, C.I., Kim, J.-H., Schouten, S., Sinninghe Damsté, J.S., 2014b. Occurrence and abundance of 6-methyl branched glycerol dialkyl glycerol tetraethers in soils: Implications for palaeoclimate reconstruction. Geochimica et Cosmochimica Acta 141, 97–112.

De Jonge, C. Stadnitskaia, A., Hopmans, E.C., Cherkashov, G., Fedotov, A., Streletskaya, I.D., Vasiliev, A., Sinninghe Damsté, J.S. Drastic changes in the distribution of branched tetraether lipids in suspended matter and sediments from the Yenisei River and Kara Sea (Siberia): Implications for the use of brGDGT-based proxies in coastal marine sediments. Submitted to Geochimica et Cosmochimica Acta.

Fietz, S., Martínez-Garcia, A., Huguet, C., Rueda, G., Rosell-Melé, A., 2011. Constraints in the application of the Branched and Isoprenoid Tetraether index as a terrestrial input proxy. Journal of Geophysical Research: Oceans 116, C10032.

Hopmans, E.C., Weijers, J.W.H., Schefuß, E., Herfort, L., Sinninghe Damsté, J.S., Schouten, S., 2004. A novel proxy for terrestrial organic matter in sediments based on branched and isoprenoid tetraether lipids. Earth and Planetary Science Letters 224, 107–116.

Huguet, C., Hopmans, E.C., Febo-Ayala, W., Thompson, D.H., Sinninghe Damsté, J.S., Schouten, S., 2006. An improved method to determine the absolute abundance of glycerol dibiphytanyl glycerol tetraether lipids. Organic Geochemistry 37, 1036–1041.

Jewell, W.J., McCarty, P.L., 1971. Aerobic decomposition of algae. Environmental Science and Technology 5, 1023–1031.

Kim, J.-H., Zell, C., Moreira-Turcq, P., Perez, M.A.P., Abril, G., Mortillaro, J.-M., Weijers, J.W.H., Meziane, T., Sinninghe Damsté, J.S., 2012. Tracing soil organic carbon in the lower Amazon River and its tributaries using GDGT distributions and bulk organic matter properties. Geochimica et Cosmochimica Acta 90, 163–180.

Lliros, M., Gich, F., Plasencia, A., Auguet, J.-C., Darchambeau, F., Casamayor, E.O., Descy, J.-P., Borrego, C., 2010. Vertical distribution of ammonia-oxidizing Crenarchaeota and methanogens in the epipelagic waters of Lake Kivu (Rwanda-Democratic Republic of the Congo). Applied and Environmental Microbiology 76, 6853–6863.

Loomis, S.E., Russell, J.M., Sinninghe Damsté, J.S., 2011. Distributions of branched GDGTs in soils and lake sediments from western Uganda: Implications for a lacustrine paleothermometer. Organic Geochemistry 42, 739–751.

Loomis, S.E., Russell, J.M., Ladd, B., Street-Perrott, F.A., Sinninghe Damsté, J.S., 2012. Calibration and application of the branched GDGT temperature proxy on East African lake sediments. Earth and Planetary Science Letters 357-358, 277–288.

Loomis, S.E., Russell, J.M., Eggermont, H., Verschuren, D., Sinninghe Damsté, J.S., 2014a. Effects of temperature, pH and nutrient concentration on branched GDGT distributions in East African lakes: Implications for paleoenvironmental reconstruction. Organic Geochemistry 66, 25–37.

Loomis, S.E., Russell, J.M., Heureux, A.M., D'Andrea, W.J., Sinninghe Damsté, J.S., 2014b. Seasonal variability of branched glycerol dialkyl glycerol tetraethers (brGDGTs) in a temperate lake system. Geochimica et Cosmochimica Acta 144, 173-187.

Maksimenko, S.Y., Zemskaya, T.I., Pavlova, O.N., Ivanov, V.G., Buryukhaev, S.P., 2008. Microbial community of the water column of the Selenga River-Lake Baikal biogeochemical barrier. Microbiology 77, 587–594.

Michener R. H. and Lajtha K. (Eds) 2007. Stable isotopes in ecology and environmental science., Blackwell Scientific Publications, Oxford, UK.

Niemann, H., Stadnitskaia, A., Wirth, S.B., Gilli, A., Anselmetti, F.S., Sinninghe Damsté, J.S., Schouten, S., Hopmans, E.C., Lehmann, M.F., 2012. Bacterial GDGTs in Holocene sediments and catchment soils of a high Alpine lake: application of the MBT/CBT-paleothermometer. Climate of the Past 8, 889–906.

Pancost, R.D., Sinninghe Damsté, J.S., 2003. Carbon isotopic compositions of prokaryotic lipids as tracers of carbon cycling in diverse settings. Chemical Geology 195, 29–58.

Pearson, A., Huang, Z., Ingalls, A.E., Romanek, C.S., Wiegel, J., Freeman, K.H., Smittenberg, R.H., Zhang, C.L., 2004. Nonmarine Crenarchaeol in Nevada Hot Springs. Applied Environmental Microbiology 70, 5229–5237.

Pearson, E.J., Juggins, S., Talbot, H.M., Weckstrom, J., Rosen, P., Ryves, D.B., Roberts, S.J., Schmidt, R., 2011. A lacustrine GDGT-temperature calibration from the Scandinavian Arctic to Antarctic: Renewed potential for the application of GDGT-paleothermometry in lakes. Geochimica et Cosmochimica Acta 75, 6225–6238.

Peterse, F., Nicol, G.W., Schouten, S., Sinninghe Damsté, J.S., 2010. Influence of soil pH on the abundance and distribution of core and intact polar lipid-derived branched GDGTs in soil. Organic Geochemistry 41, 1171–1175.

Peterse, F., Prins, M.A., Beets, C.J., Troelstra, S.R., Zheng, H., Gu, Z., Schouten, S., Sinninghe Damsté, J.S., 2011. Decoupled warming and monsoon precipitation in East Asia over the last deglaciation. Earth and Planetary Science Letters 301, 256–264.

Pitcher, A., Hopmans, E.C., Schouten, S., Sinninghe Damsté, J.S., 2009. Separation of core and intact polar archaeal tetraether lipids using silica columns: Insights into living and fossil biomass contributions. Organic Geochemistry 40, 12–19.

Pouliot, J., Galand, P.E., Lovejoy, C., Vincent, W.F., 2009. Vertical structure of archaeal communities and the distribution of ammonia monooxygenase A gene variants in two meromictic High Arctic lakes. Environmental Microbiology 11, 687–699.

Schoon, P.L., de Kluijver, A., Middelburg, J.J., Downing, J.A., Sinninghe Damsté, J.S., Schouten, S., 2013. Influence of lake water pH and alkalinity on the distribution of core and intact polar branched glycerol dialkyl glycerol tetraethers (GDGTs) in lakes. Organic Geochemistry 60, 72–82.

Schouten, S., Hopmans, E.C., Pancost, R.D., Sinninghe Damsté, J.S., 2000. Widespread occurrence of structurally diverse tetraether membrane lipids: Evidence for the ubiquitous presence of low-temperature relatives of hyperthermophiles. Proceedings of the National Academy of Sciences USA 97, 14421–14426.

Schouten, S., Huguet, C., Hopmans, E.C., Kienhuis, M.V.M., Sinninghe Damsté, J.S., 2007. Analytical methodology for TEX_{86} paleothermometry by high-performance liquid chromatography/atmospheric pressure chemical ionization-mass spectrometry. Analytical Chemistry 79, 2940–2944.

Schouten, S., Hopmans, E.C., van der Meer, J., Mets, A., Bard, E., Bianchi, T.S., Diefendorf, A., Escala, M., Freeman, K.H., Furukawa, Y., Huguet, C., Ingalls, A., Menot-Combes, G., Nederbragt, A.J., Oba, M., Pearson, A., Pearson, E.J., Rosell-Mele, A., Schaeffer, P., Shah, S.R., Shanahan, T.M., Smith, R.W., Smittenberg, R., Talbot, H.M., Uchida, M., Van Mooy, B.A.S., Yamamoto, M., Zhang, Z.H., Sinninghe Damsté, J.S., 2009. An interlaboratory study of TEX_{86} and BIT analysis using high-performance liquid chromatography-mass spectrometry. Geochemistry Geophysics Geosystems 10, 13.

Schouten, S., Rijpstra, W.I.C., Durisch-Kaiser, E., Schubert, C.J., Sinninghe Damsté, J.S., 2012. Distribution of glycerol dialkyl glycerol tetraether lipids in the water column of Lake Tanganyika. Organic Geochemistry 53, 34–37.

Schouten, S., Hopmans, E.C., Rosell-Melé, A., Pearson, A., Adam, P., Bauersachs, T., Bard, E., Bernasconi, S.M., Bianchi, T.S., Brocks, J.J., Carlson, L.T., Castañeda, I.S., Derenne, S., Selver, A.D., Dutta, K., Eglinton, T., Fosse, C., Galy, V., Grice, K., Hinrichs, K.-U., Huang, Y., Huguet, A., Huguet, C., Hurley, S., Ingalls, A., Jia, G., Keely, B., Knappy, C., Kondo, M., Krishnan, S., Lincoln, S., Lipp, J., Mangelsdorf, K., Martínez-García, A., Ménot, G., Mets, A., Mollenhauer, G., Ohkouchi, N., Ossebaar, J., Pagani, M., Pancost, R.D., Pearson, E.J., Peterse, F., Reichart, G.-J., Schaeffer, P., Schmitt, G., Schwark, L., Shah, S.R., Smith, R.W., Smittenberg, R.H., Summons, R.E., Takano, Y., Talbot, H.M., Taylor, K.W.R., Tarozo, R., Uchida, M., van Dongen, B.E., Van Mooy, B.A.S., Wang, J., Warren, C., Weijers, J.W.H., Werne, J.P., Woltering, M., Xie, S., Yamamoto, M., Yang, H., Zhang, C.L., Zhang, Y., Zhao, M., Sinninghe Damsté, J.S., 2013. An interlaboratory study of TEX_{86} and BIT analysis of sediments, extracts, and standard mixtures. Geochemistry Geophysics Geosystems 14, 5263–5285.

Sinninghe Damsté, J.S., Hopmans, E.C., Pancost, R.D., Schouten, S., Geenevasen, J.A.J., 2000. Newly discovered non-isoprenoid glycerol dialkyl glycerol tetraether lipids in sediments. Chemical Communications 1683–1684.

Sinninghe Damsté, J.S., Schouten, S., Hopmans, E.C., van Duin, A.C.T., Geenevasen, J.A.J., 2002. Crenarchaeol: the characteristic core glycerol dibiphytanyl glycerol tetraether membrane lipid of cosmopolitan pelagic crenarchaeota. Journal of Lipid Research 43, 1641–1651.

Sinninghe Damsté, J.S., Ossebaar, J., Abbas, B., Schouten, S., Verschuren, D., 2009. Fluxes and distribution of tetraether lipids in an equatorial African lake: Constraints on the application of the TEX_{86} palaeothermometer and BIT index in lacustrine settings. Geochimica et Cosmochimica Acta 73, 4232–4249.

Sinninghe Damsté, J.S., Rijpstra, W.I.C., Hopmans, E.C., Weijers, J.W.H., Foesel, B.U., Overmann, J., Dedysh, S.N., 2011. 13, 16-dimethyloctacosanedioic acid (iso-diabolic acid), a common membrane-spanning lipid of Acidobacteria subdivisions 1 and 3. Applied and Environmental Microbiology 77, 4147–4154.

Sinninghe Damsté, J.S., Rijpstra, W.I.C., Hopmans, E.C., Foesel, B.U., Wüst, P.K., Overmann, J., Tank, M., Bryant, D.A., Dunfield, P.F., Houghton, K., Stott, M.B., 2014. Ether- and ester-bound iso-diabolic acid and other lipids in members of Acidobacteria subdivision 4. Applied and Environmental Microbiology 80, 5207-5218.

Sorokovikova, L.M., Popovskaya, G.I., Belykh, O.I., Tomberg, I.V., Maksimenko, S.Y., Bashenkhaeva, N.V., Ivanov, V.G., Zemskaya, T.I., 2012. Plankton composition and water chemistry in the mixing zone of the Selenga River with Lake Baikal. Hydrobiologia 695, 329–341.

Sun, Q., Chu, G.Q., Liu, M.M., Xie, M.M., Li, S.Q., Ling, Y.A., Wang, X.H., Shi, L.M., Jia, G.D., Lu, H.Y., 2011. Distributions and temperature dependence of branched glycerol dialkyl glycerol tetraethers in recent lacustrine sediments from China and Nepal. Journal of Geophysical Research-Biogeosciences 116, 1-12.

Tierney, J.E., Russell, J.M., 2009. Distributions of branched GDGTs in a tropical lake system: Implications for lacustrine application of the MBT/CBT paleoproxy. Organic Geochemistry 40, 1032–1036.

Tierney, J.E., Russell, J.M., Eggermont, H., Hopmans, E.C., Verschuren, D., Sinninghe Damsté, J.S., 2010. Environmental controls on branched tetraether lipid distributions in tropical East African lake sediments. Geochimica et Cosmochimica Acta 74, 4902–4918.

Tierney, J.E., Schouten, S., Pitcher, A., Hopmans, E.C., Sinninghe Damsté, J.S., 2012. Core and intact polar glycerol dialkyl glycerol tetraethers (GDGTs) in Sand Pond, Warwick, Rhode Island (USA): Insights into the origin of lacustrine GDGTs. Geochimica et Cosmochimica Acta 77, 561–581.

Votintsev, K.K., 1985. Main features of the hydrochemistry of Lake Baikal. Water Resources 12, 106–116.

Votintsev, K.K., Mescheryakova, A.I., Popovskaya, G.I., 1975. Cycle of Organic Matter in Lake Baikal. Nauka, Novosibirsk.

Weijers, J.W.H., Schouten, S., Hopmans, E.C., Geenevasen, J.A.J., David, O.R.P., Coleman, J.M., Pancost, R.D., Sinninghe Damsté, J.S., 2006. Membrane lipids of mesophilic anaerobic bacteria thriving in peats have typical archaeal traits. Environmental Microbiology 8, 648–657.

Weijers, J.W.H., Schouten, S., van den Donker, J.C., Hopmans, E.C., Sinninghe Damsté, J.S., 2007. Environmental controls on bacterial tetraether membrane lipid distribution in soils. Geochimica et Cosmochimica Acta 71, 703–713.

Weijers, J.W.H., Schefuss, E., Schouten, S., Sinninghe Damsté, J.S., 2007. Coupled thermal and hydrological evolution of tropical Africa over the last deglaciation. Science 315, 1701–1704.

Weijers, J.W.H., Panoto, E., van Bleijswijk, J., Schouten, S., Rijpstra, W.I.C., Balk, M., Stams, A.J.M., Sinninghe Damsté, J.S., 2009. Constraints on the biological source(s) of the orphan branched tetraether membrane lipids. Geomicrobiology Journal 26, 402–414.

Weijers, J.W.H., Wiesenberg, G.L.B., Bol, R., Hopmans, E.C., Pancost, R.D., 2010. Carbon isotopic composition of branched tetraether membrane lipids in soils suggest a rapid turnover and a heterotrophic life style of their source organism(s). Biogeosciences 7, 2959–2973.

Woltering, M., Werne, J.P., Kish, J.L., Hicks, R., Sinninghe Damsté, J.S., Schouten, S., 2012. Vertical and temporal variability in concentration and distribution of thaumarchaeotal tetraether lipids in Lake Superior and the implications for the application of the TEX_{86}temperature proxy. Geochimica et Cosmochimica Acta 87, 136–153.

Yoshii, K., 1999. Stable isotope analyses of benthic organisms in Lake Baikal. Hydrobiologia 411, 145–159.

Yoshii, K., Melnik, N.G., Timoshkin, O.A., Bondarenko, N.A., Anoshko, P.N., Yoshioka, T., Wada, E., 1999. Stable isotope analyses of the pelagic food web in Lake Baikal. Limnology and Oceanography 44, 502–511.

Zell, C., Kim, J.-H., Moreira-Turcq, P., Abril, G., Hopmans, E.C., Bonnet, M.-P., Sobrinho, R.L., Sinninghe Damsté, J.S., 2013. Disentangling the origins of branched tetraether lipids and crenarchaeol in the lower Amazon River: Implications for GDGT-based proxies. Limnology and Oceanography 58, 343–353.

Zell, C., Kim, J.-H., Balsinha, M., Dorhout, D., Fernandes, C., Baas, M., Sinninghe Damsté, J.S., 2014. Transport of branched tetraether lipids from the Tagus River basin to the coastal ocean of the Portuguese margin: consequences for the interpretation of the MBT'/CBT paleothermometer. Biogeosciences 11, 5637-5655.

Tables

Table 1

Sampling station data (n.d., not determined; n.a., not available).

Site	Latitude (°N)	Longitude (°E)	Depth bsl (m)[a]	Distance SRM (km)[b]	Sampling date	Measured pH	Measured temp (°C)	POC (mg/l)	$\delta^{13}C_{POC}$ (‰)
SR[c]	51.72833	107.4628	0.5	-150	06-07-2010	8.4	25.0	6.4	-27.0
SRM	52.27318	106.2547	0.5	0	20-07-2010	8.1	22.5	5.9	-28.4
S1	52.27852	106.2444	0.5	1	20-07-2010	8.1	15.0	5.1	-28.8
S3	52.29025	106.2226	0.5	3	22-07-2010	8.1	13.0	2.0	-28.4
S5	52.30313	106.1998	0.5	5	28-07-2010	8.0	11.3	1.5	-28.2
B1	52.27852	106.2444	6	1	20-07-2010	7.9	9.3	2.5	-28.8
B3	52.29025	106.2226	17	3	20-07-2010	7.9	6.6	1.1	-29.0
B5	52.30313	106.1998	25	5	28-07-2010	8.0	5.2	1.3	-29.3
Ba	51.89194	104.8233	0.5	105	01-07-2010	8.8	6.7	1.3	-24.0
MIR[c]	51.94533	100.78839	0.5	n.a.	11-07-2010	5.6	10.8	0.1	-27.3
Y1[c]	58.00992	93.11680	2.0	n.a.	25-8-2009	n.d.	12.0	0.03	b.d.l.
Y2[c]	58.13147	92.75405	3.0	1500	29-9-2009	n.d.	11.0	0.09	-30.3

[a] Below surface water level; [b] estimated downstream distance relative to Selenga River mouth, so upstream samples thus have negative values,[c] samples reported by De Jonge et al., 2014b and De Jonge et al., submitted.

Table 2

Fractional abundance (% of total) and concentrations of CL brGDGTs and crenarchaeol in SPM of Selenga River and its outflow into Lake Baikal, in the Mountainous Irkut River and in the Yenisei River (b.d.l., below detection limit).

Site	Fractional abundance (%)														BrGDGTs	Crenarchaeol	IR	BIT	pH[a]	MST[a]
	Ia	Ib	Ic		IIb		IIIa	IIIb	IIIc	IIa'	IIb'	IIc'	IIIa'	IIIb'	IIIc'	(µg/g POC)	(µg/g POC)				(°C)
SR[b]	12	5	1	0.68	4	7.5	8	0.4	b.d.l	24	7	0.4	24	1	b.d.l	4	0.2	0.68	0.93	7.5	20
SRM	13	5	1	0.71	3	7.5	7	0.3	0.1	25	8	0.3	23	1	0.3	12	0.4	0.71	0.96	7.5	20
S1	14	5	1	0.70	3	7.5	8	0.4	0.05	25	7	0.3	21	1	0.3	10	0.4	0.70	0.96	7.5	19
S3	17	7	1	0.56	5	7.1	12	b.d.l	b.d.l	18	6	b.d.l	19	b.d.l	b.d.l	1	0.4	0.56	0.71	7.1	20
S5	18	5	b.d.l	0.52	4	7.0	16	b.d.l	b.d.l	17	5	b.d.l	17	b.d.l	b.d.l	0.6	0.6	0.52	0.45	7.0	18
B1	14	6	1	0.56	4	7.2	12	0.5	b.d.l	20	6	0.3	18	1	b.d.l	6	0.9	0.56	0.84	7.2	19
B3	16	4	1	0.43	3	6.5	23	0.4	b.d.l	11	3	b.d.l	11	1	b.d.l	10	2.7	0.43	0.77	6.5	15
B5	12	5	2	0.45	6	6.9	23	1	0.3	11	4	0.4	17	1	1	2	0.8	0.45	0.63	6.9	17
Ba	10	2	b.d.l	0.44	2	7.0	26	b.d.l	b.d.l	10	1	b.d.l	32	b.d.l	b.d.l	0.1	0.2	0.44	0.22	7.0	14
MIR[b]	11	2	0.4	0.51	2	6.9	24	0.3	b.d.l	15	2	0.3	20	1	b.d.l	15	0.1	0.51	0.99	6.9	13
Y1[b]	14	3	1	0.71	2	7.5	9	0.4	0.1	18	3	b.d.l.	36	1	0.1	10	0.3	0.71	0.97	7.5	18
Y2[b]	9	3	0.4	0.80	2	7.9	7	0.4	0.1	19	7	0.2	42	2	0.4	21	0.2	0.80	0.99	7.9	19

[a] reconstructed pH and MST; [b] reported by De Jonge et al., 2014b and De Jonge et al., submitted.

Figure captions

Fig. 1. Chemical structures of branched GDGTs (I-III) and crenarchaeol (IV). The chemical structures of the hexa- and pentamethylated brGDGTs with cyclopentyl moiety(ies) IIb', IIc', IIIb' and IIIc' are tentatively assigned.

Fig. 2. Map of the Southern part of Lake Baikal, with the sample sites indicated. Insert **a** shows the distribution of the SPM samples collected in the Selenga River outflow. Insert **b** shows, i) the extent of the watershed of Lake Baikal, where all rivers that drain into Lake Baikal are indicated in orange and ii) the Southern part of the Yenisei River watershed, where all rivers that drains into the Yenisei River (and the Yenisei River itsself) are indicated in blue.

Fig. 3. Figure plotting the environmental variables of Lake Baikal and its inflowing rivers; measured water temperature (°C, A), measured water pH (B), measured concentration of POC (μg/l, C) and the stable carbon isotopic value of the bulk OM, $\delta^{13}C_{POC}$ (‰, D). The shaded areas indicate riverine samples, where orange denotes the Selenga River, and grey denotes the Irkut River. Surface water is indicated by round symbols, bottom water is indicated with triangles. Please note that the x-axis, where the distance to the Selenga River Mouth is plotted is broken, as to allow the Selenga River, the Lake Baikal sample and the Mountain River to be plotted on the same axis. Selenga outflow samples, collected in the same sampling campaign, are connected.

Fig. 4. The concentration of CL brGDGTs (μg/g POC, A) and crenarchaeol (μg/g POC, B) and the BIT-index values (C), in Lake Baikal and its inflowing rivers. The shaded areas indicate riverine samples, where orange denotes the Selenga River, and grey denotes the Irkut River. Surface water is indicated by round symbols, bottom water is indicated with triangles. Please note that the x-axis, where the distance to the Selenga River Mouth is plotted is broken, as to allow the Selenga River, the Lake Baikal sample and the mountainous Irkut River to be plotted on the same axis. Selenga outflow samples, collected in the same sampling campaign, are connected.

Fig. 5. The fractional abundance (FA), expressed as the percentage of the total of the 15 brGDGT compounds, of the CL (A-F) fraction of selected samples: Selenga River Mouth (SRM, A), the surface water at 3 km distance from the outflow (S3, B), the bottom water at 3 km from the outflow (B3, C), the bottom water at 5 km from the outflow (B5, D), the shoreline Lake Baikal setting (Ba, E), the Mountainous Irkut River (IR, F), the Yenisei River

before (Y1, G) and after the Angara River inflow (Y2, H). The color of the bars refers to the structure of the brGDGTs, and is referred to in the legend.

Fig. 6. PCA based on the standardized fractional abundances of the Lake Baikal brGDGTs and the inflowing Selenga and Irkut Rivers. Panel A and B plot principal component 1 (PC1) against PC2, panel C and D plots PC1 against PC3. The scores of the brGDGT compounds are indicated in panel A and C, and the scores of the sites are plotted in panels B and D. Surface waters are indicated with round symbols and connected with the corresponding bottom waters (triangular symbol) with a grey line. The correlation of the measured water temperature (Temp) with the PCs is plotted *a posteriori* in the ordination space (panel B), indicated with a dotted line.

Fig. 7. Truncated triplot, based on the fractional abundances of the brGDGTs Ia, IIIa and IIIa'. The sum of the fractional abundances amounts up to 100%. The round symbols indicate surface water of Lake Baikal and inflowing rivers. The triangles indicate Lake Baikal bottom waters, while the diamonds indicate the brGDGT distribution in the Yenisei River. The full black line covers brGDGT distributions that can be explained by linear mixing between the Selenga River Mouth (SRM) distribution and the Baikal outflow (Ba) distributions. The dotted line covers brGDGT distributions that can be explained by linear mixing between the Selenga River Mouth (SRM) distribution and the mountainous Irkut River (MIR) distributions.

Fig. 8. The isomer ratio IR [Eq. 1] (A), the reconstructed MST [Eq. 5] (B) and the reconstructed pH [Eq. 3 and 4] (C) are plotted. The shaded areas indicate riverine samples, where orange denotes the Selenga River, and grey denotes the mountainous Irkut River. Surface water is indicated by round symbols, bottom water is indicated with triangles. Please note that athe x-axis, where the distance to the Selenga River Mouth is plotted is broken, as to allow the Selenga River, the Lake Baikal sample and the Mountain River to be plotted on the same axis. Selenga outflow samples, collected in the same sampling campaign, are connected.

Ia
m/z 1022

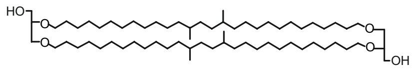

Ib
m/z 1020

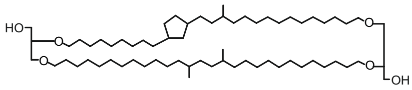

Ic
m/z 1018

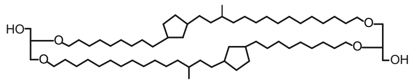

IIa
m/z 1036

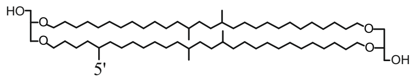

IIa’
m/z 1036

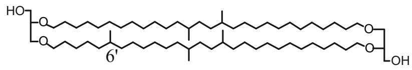

IIb
m/z 1034

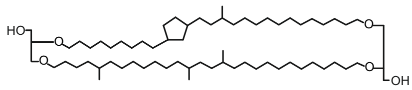

IIb’
m/z 1034

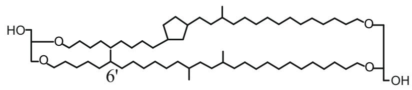

IIc
m/z 1032

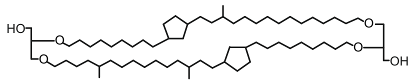

IIc’
m/z 1032

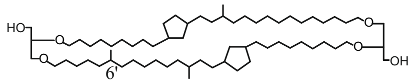

IIIa
m/z 1050

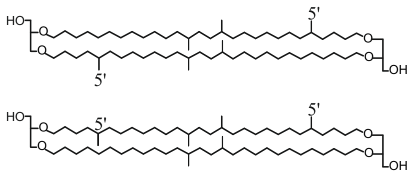

IIIa’
m/z 1050

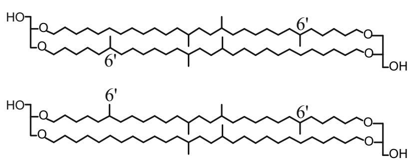

IIIb
m/z 1048

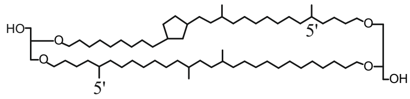

IIIb’
m/z 1048

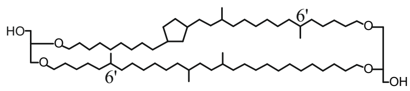

IIIc
m/z 1046

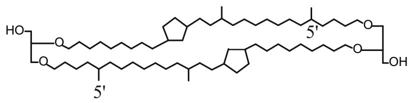

IIIc’
m/z 1046

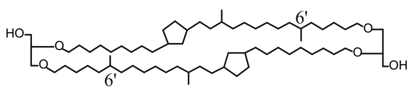

IV
m/z 1292

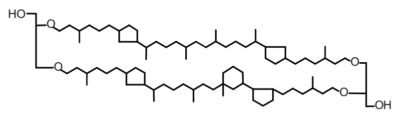

Fig. 1

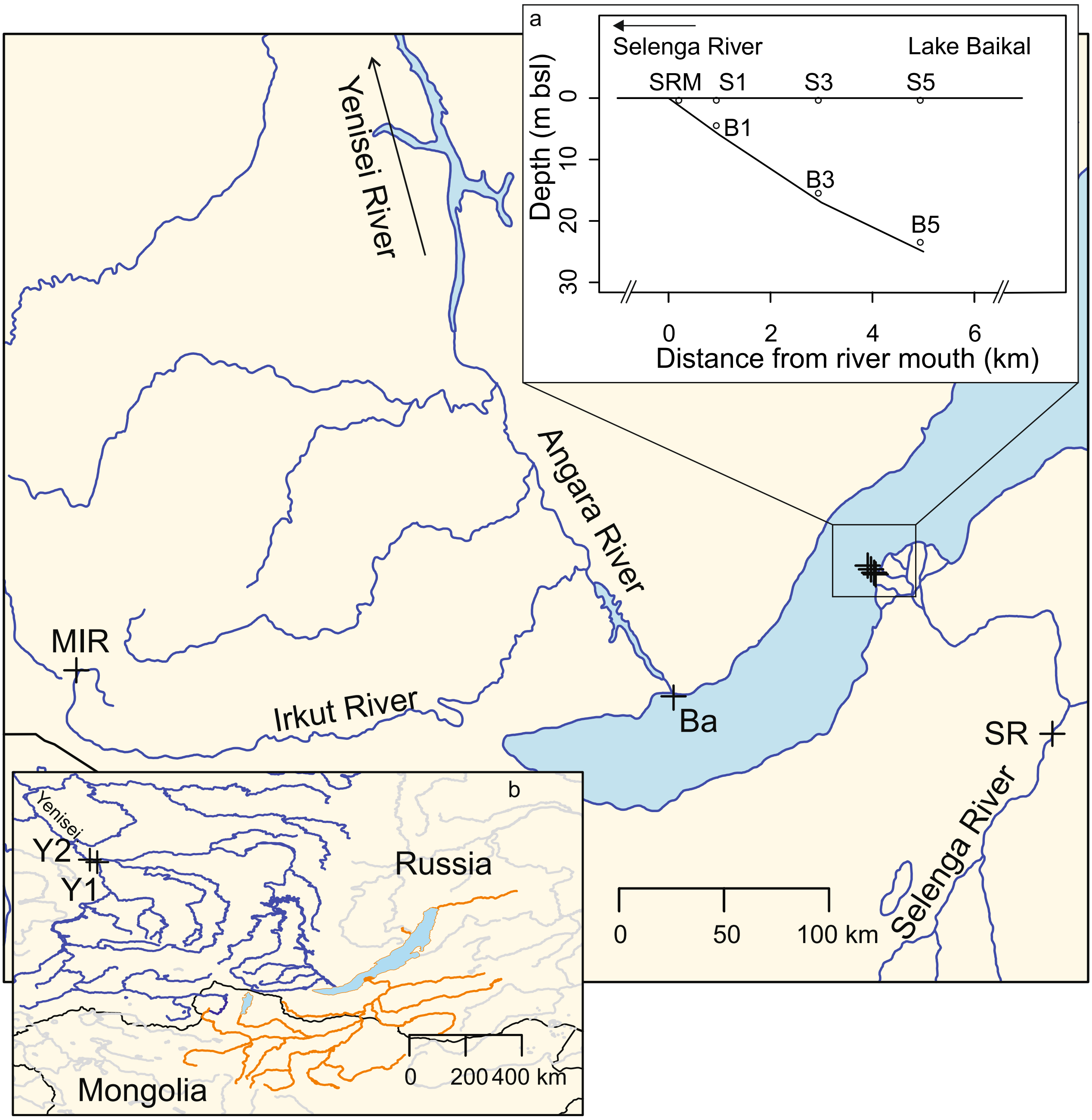

a
Selenga River
Lake Baikal
SRM
S1
S3
S5
B1
B3
B5
Depth (m bsl)
0
10
20
30
0
2
4
6
Distance from river mouth (km)
Yenisei River
Angara River
Irkut River
MIR
Ba
SR
Selenga River
0
50
100 km
b
Yenisei
Y2
Y1
Russia
Mongolia
0
200
400 km

Fig. 2

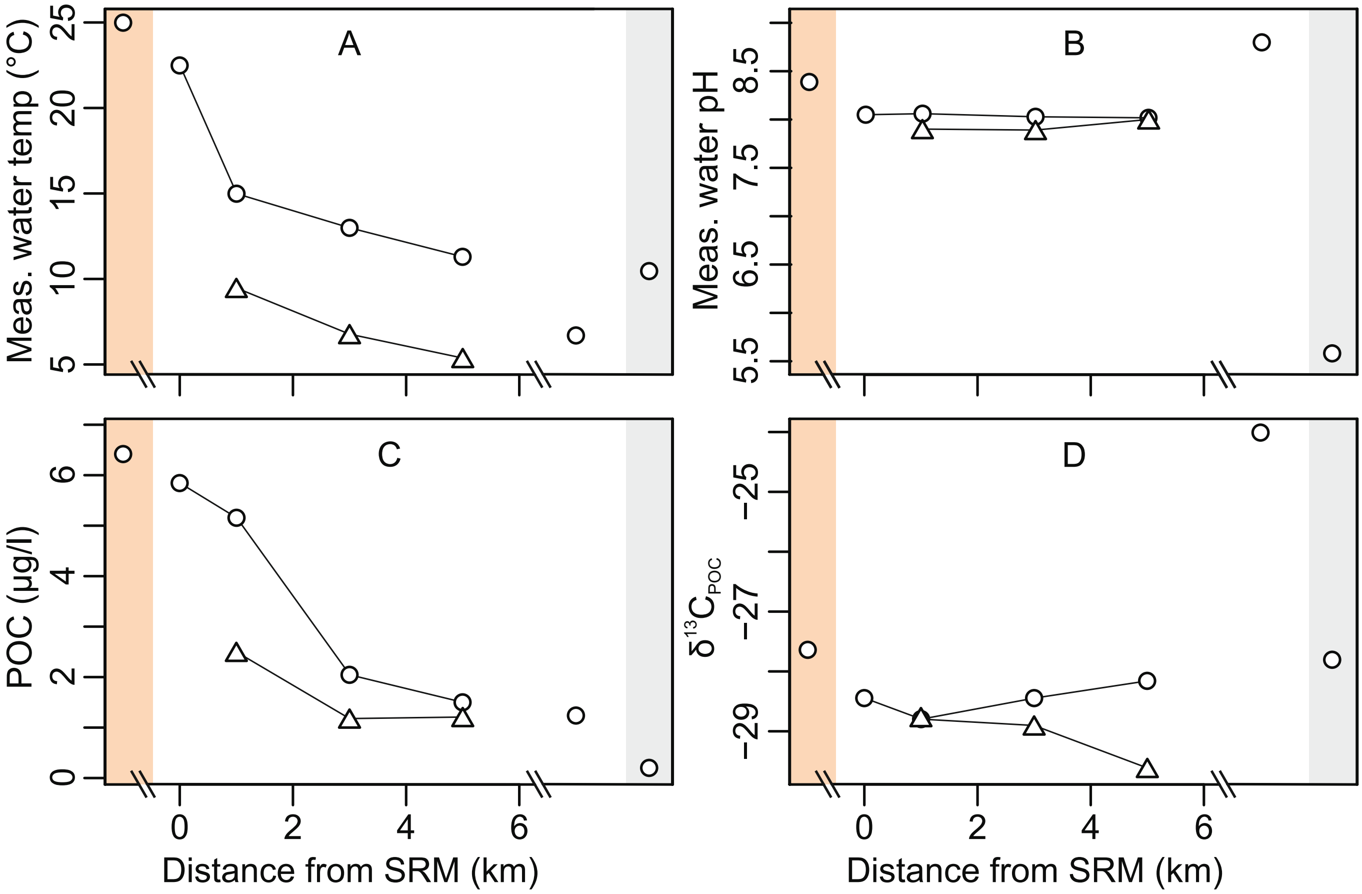
A
B
C
D
Meas. water temp (°C)
Meas. water pH
POC (µg/l)
δ13CPOC
Distance from SRM (km)
Distance from SRM (km)
25
20
15
10
5
8.5
7.5
6.5
5.5
6
4
2
0
−25
−27
−29
0
2
4
6

Fig. 3

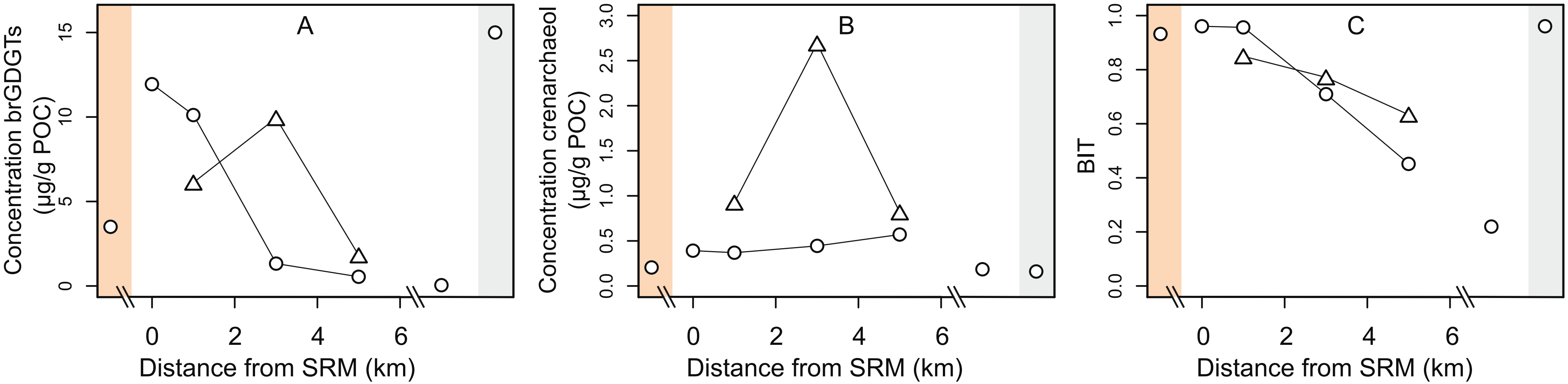

A
Concentration brGDGTs
(µg/g POC)
0
5
10
15
0
2
4
6
Distance from SRM (km)
B
Concentration crenarchaeol
(µg/g POC)
0.0
0.5
1.0
1.5
2.0
2.5
3.0
0
2
4
6
Distance from SRM (km)
C
BIT
0.0
0.2
0.4
0.6
0.8
1.0
0
2
4
6
Distance from SRM (km)

Fig. 4

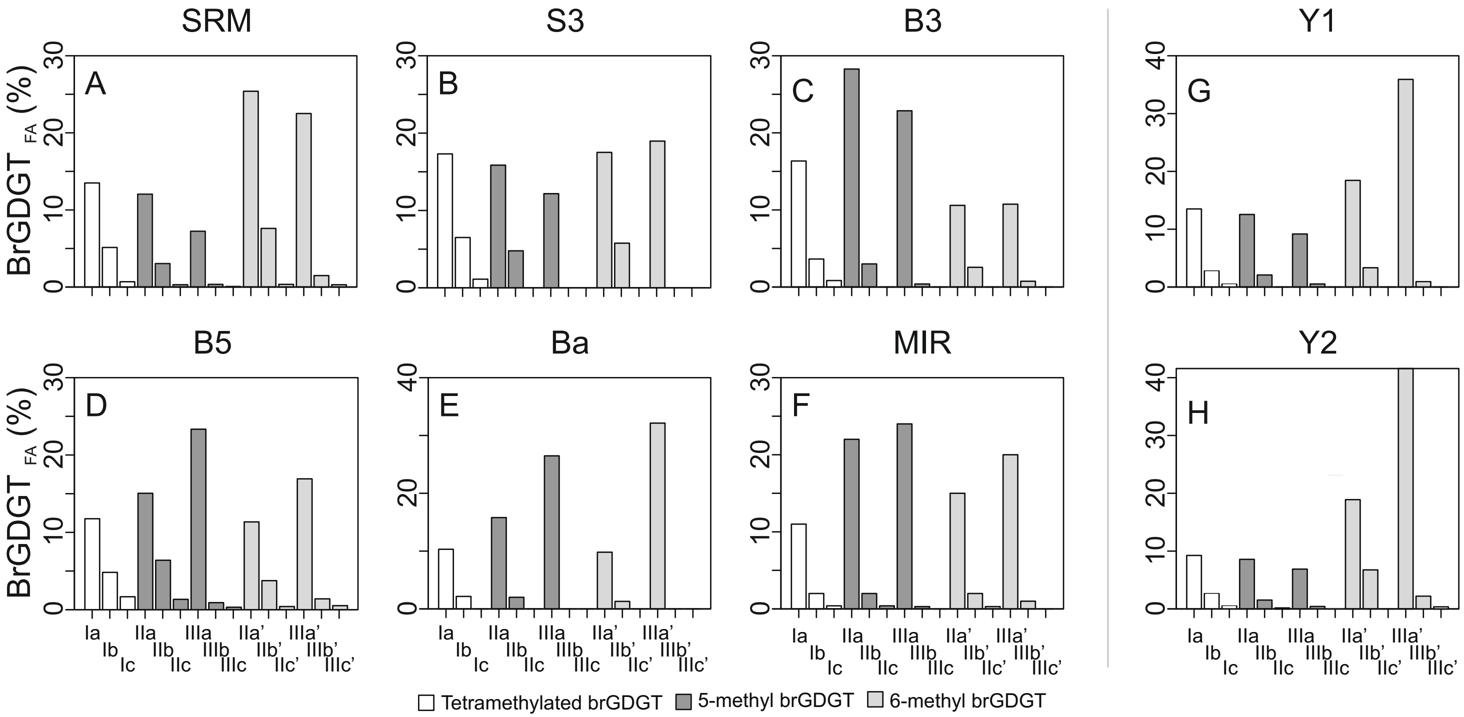
SRM
S3
B3
Y1
B5
Ba
MIR
Y2
A
B
C
D
E
F
G
H
BrGDGT FA (%)
Ia
Ib
Ic
IIa
IIb
IIc
IIIa
IIIb
IIIc
IIa'
IIb'
IIc'
IIIa'
IIIb'
IIIc'
Tetramethylated brGDGT
5-methyl brGDGT
6-methyl brGDGT

Fig. 5

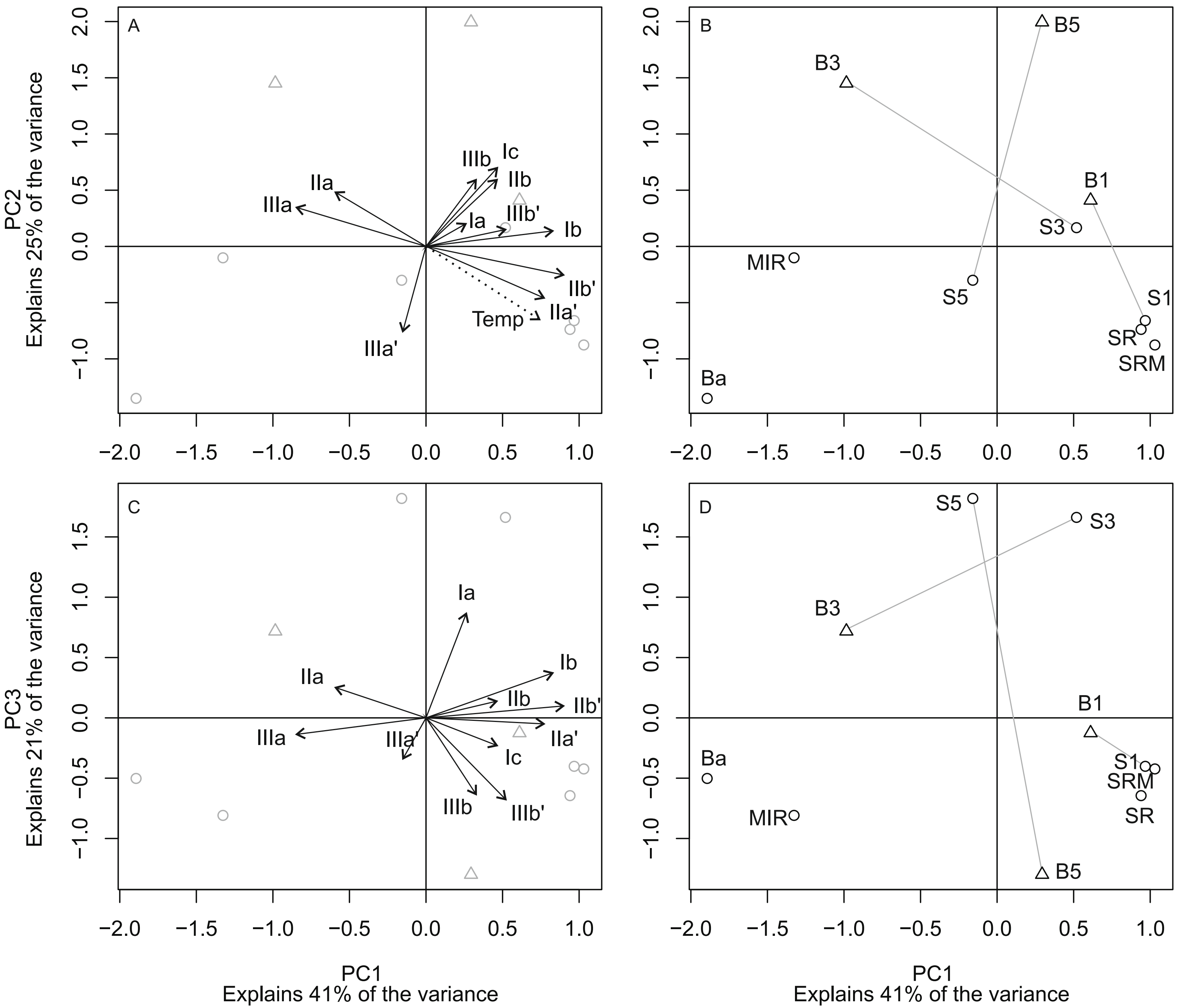
A
B
C
D
IIIb
Ic
IIb
IIa
IIIa
Ia
IIIb'
Ib
IIb'
IIa'
Temp
IIIa'
B5
B3
B1
S3
MIR
S5
S1
SR
SRM
Ba
PC1
Explains 41% of the variance
PC2
Explains 25% of the variance
PC3
Explains 21% of the variance

Fig. 6

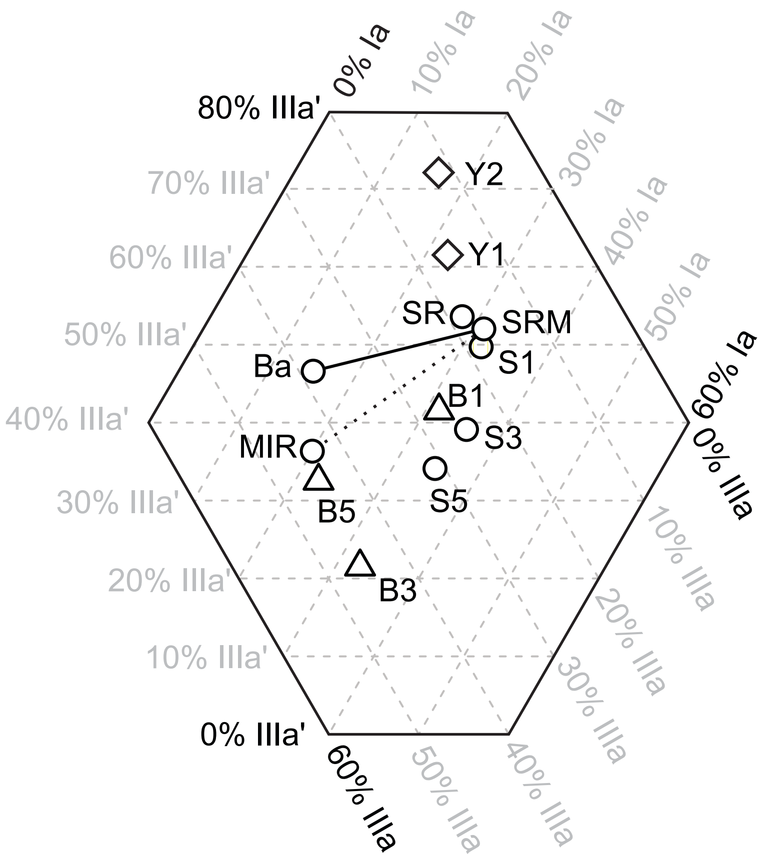

0% Ia
10% Ia
20% Ia
30% Ia
40% Ia
50% Ia
60% Ia
0% IIIa
10% IIIa
20% IIIa
30% IIIa
40% IIIa
50% IIIa
60% IIIa
80% IIIa'
70% IIIa'
60% IIIa'
50% IIIa'
40% IIIa'
30% IIIa'
20% IIIa'
10% IIIa'
0% IIIa'
Y2
Y1
SR
SRM
S1
Ba
B1
S3
MIR
S5
B5
B3

Fig. 7

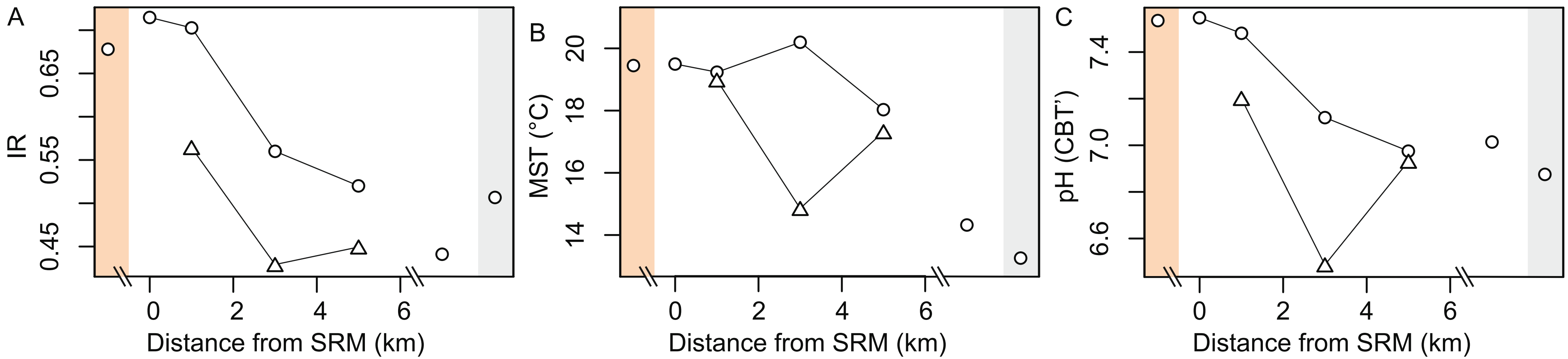
A
IR
0.45
0.55
0.65
0
2
4
6
Distance from SRM (km)
B
MST (°C)
14
16
18
20
0
2
4
6
Distance from SRM (km)
C
pH (CBT')
6.6
7.0
7.4
0
2
4
6
Distance from SRM (km)

Fig. 8